Modeling Two-Dimensional Material-Based Photodetectors with Finite-Difference Methods

Raonaqul Islam
Department of Computer Science & Electrical Engineering
University of Maryland Baltimore County
Baltimore, MD, USA
raonaqul.islam@umbc.edu

Ergun Simsek
Department of Computer Science & Electrical Engineering
University of Maryland Baltimore County
Baltimore, MD, USA
simsek@umbc.edu

***Abstract*—We developed a finite-difference frequency-domain (FDFD) and a finite-difference time-domain (FDTD) drift-diffusion equations solver that takes the multilayered background into account for realistic characterization. Comparisons between the numerical results and experiments validate the accuracy of the proposed approach in calculating the output current, quantum efficiency, and phase noise of the photodetector as a function of incident wavelength.**

***Index Terms*—drift-diffusion, photodetector, two-dimensional materials.**

I. Introduction

In the last two decades, we have witnessed a growing interest in two-dimensional (2D) materials, specifically monolayers and few-layers of transition metal dichalcogenides (TMDs), owing to their remarkable electrical, optical, and thermal properties and versatility in photonics and optoelectronics applications [1]–[3]. Notably, these materials, with thicknesses at the atomic scale, exhibit strong absorption characteristics within the visible part of the electromagnetic spectrum. Such attributes render them highly promising for the development of various devices, including field-effect transistors, photodiodes, light-emitting devices, and sensors [1]–[5].

This work focuses on one specific member of the TMD family, namely, the monolayer of molybdenum disulfide (MoS_2). Despite significant experimental progress in the development of photodetectors based on MoS_2, a conspicuous gap exists in the literature concerning efficient numerical modeling of these devices [6]. In response to this need, we present a compact yet accurate one-dimensional (1D) solver for drift-diffusion equations, applicable in both frequency and time domains. This solver is developed based on the finite-differences method, building upon our prior work [7]. To realistically capture the material properties of MoS_2 as functions of the local electric field, doping, and temperature, we employ previously established precise numerical material models that are created based on experimental characterizations [4], [5].

The key innovation of our numerical approach lies in its ability to efficiently simulate the behavior of MoS_2-based photodetectors, offering insights into their performance under varying conditions. This is particularly crucial given the scarcity of comprehensive numerical models in the current literature. Our method enables the exploration of diverse operating scenarios, providing a valuable tool for optimizing device design and performance.

In the subsequent sections, we provide a brief mathematical formulation of the drift-diffusion equations solver and some numerical results obtained from our simulations that are compared with experimental data available in the literature, demonstrating a good agreement.

II. Numerical Model

Fig. 1 depicts the device under consideration, where a single layer of MoS_2 is positioned atop a silicon-oxide-coated silicon substrate and illuminated from the top normally. The upper gates serve as source and drain contacts, while a third contact is established at the bottom for gating purposes.

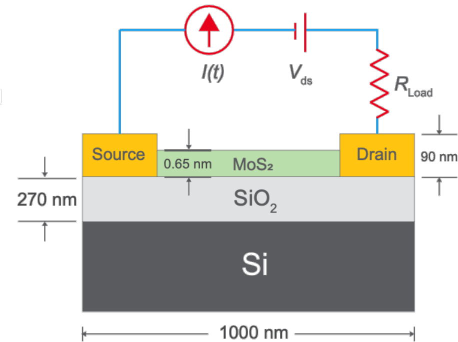

Fig. 1: Schematic illustration of the 2D material-based photodetector.

To calculate the carrier transport behavior, we solve for the drift-diffusion equations [7] that include the current continuity equations for both electrons and holes and the Poisson's equation, that are given by

$$\frac{\delta(n - N_{\mathrm{D}}^{+})}{\delta t} = G_{\mathrm{L}} - R(n,p) + \frac{\nabla \cdot \mathbf{J}_{\mathrm{n}}}{q}, \tag{1}$$

$$\frac{\delta(p - N_{\mathrm{A}}^{-})}{\delta t} = G_{\mathrm{L}} - R(n,p) + \frac{\nabla \cdot \mathbf{J}_{\mathrm{p}}}{q}, \tag{2}$$

$$\nabla \cdot \mathbf{E} = \frac{q}{\varepsilon}(N_{\mathrm{D}}^{+} + p - n - N_{\mathrm{A}}^{-}), \tag{3}$$

978-1-7335096-7-1©2024 ACES

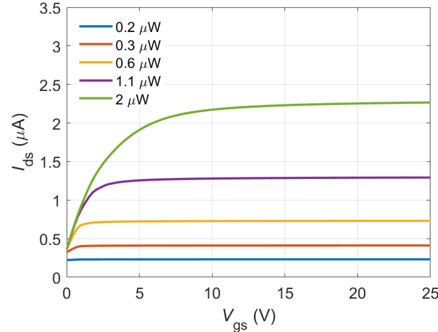

Fig. 2: Output current increases with increasing incident power.

where, q is the charge of electron, G_{L} is generation rate of the $\mathrm{MoS_2}$ layer, R is the recombination rate, ε is the permittivity of $\mathrm{MoS_2}$, and N_{D}^{+} and N_{A}^{-} are the ionized donor and acceptor impurity concentrations. $\mathbf{J}_{\mathrm{n}}$ and $\mathbf{J}_{\mathrm{p}}$ are current densities for electrons and holes, which are determined with the drift-diffusion equations:

$$\mathbf{J}_{\mathrm{n}} = qn\mathbf{v}_{\mathrm{n}}(\mathbf{E})+qD_{\mathrm{n}}\nabla n \quad \text{and} \quad \mathbf{J}_{\mathrm{p}} = qp\mathbf{v}_{\mathrm{p}}(\mathbf{E})-qD_{\mathrm{p}}\nabla p, \quad (4)$$

where, D_{n} and D_{p} are the electron and hole's diffusion coefficients, $\mathbf{v}_{\mathrm{n}}(\mathbf{E})$ and $\mathbf{v}_{\mathrm{p}}(\mathbf{E})$ are electric-field dependent electron and hole drift velocities, respectively.

To determine the complex electrical permittivity of $\mathrm{MoS_2}$ as a function of wavelength, temperature, and gating, we employed the model outlined in [4]. The evaluation of the device's load resistance (R_{Load}) involves the initial computation of the sheet resistance, $R_{\mathrm{sh}} = 1/qn\mu(T)$, for the $\mathrm{MoS_2}$ monolayer. Subsequently, this calculated value is utilized to ascertain $R_{\mathrm{Load}} = \sqrt{\rho_i \times R_{\mathrm{sh}}}$, where $\rho_i = 1/[(T-100)/107]^3$ represents the interfacial resistance between the contact and $\mathrm{MoS_2}$, with T denoting the temperature. The density of induced carriers is contingent on the thickness and properties of the oxide layer in between, expressed as $n_{\mathrm{s}} = \varepsilon_{\mathrm{ox}}(V_{\mathrm{g}} - V_{\mathrm{th}})/t_{\mathrm{ox}}$, where $\varepsilon_{\mathrm{ox}}$ denotes the permittivity of the oxide layer, t_{ox} is the oxide layer thickness, V_{th} represents the threshold voltage, and V_{g} is the applied gate voltage.

III. Numerical Results

We assume that the monolayer $\mathrm{MoS_2}$ is 0.65 nm thick and 1 μm wide. The oxide and silicon layers exhibit thicknesses of 270 nm and 2 μm, respectively. For the computation of the local electric field within the $\mathrm{MoS_2}$, we omit the source and drain contacts, and consider the bottom (gate) contact as a thin film composed of perfectly conducting material.

Fig. 2 shows the output current of the device as a function gate voltage under 5 different excitation powers for $V_{ds} = 1$ V obtained with our FDFD solver. The applied voltages are $V_{\mathrm{ds}} = -0.5$ V and $V_{\mathrm{g}} = 10$ V. In Fig. 3, we plot the quantum efficiency, phase noise, and output current of the device for varying illumination wavelengths. The red dots on the top figure are experimental results [1] of which the reported implementation is ranged within $\pm 5\%$. Note that the wavelengths where the quantum efficiency is highest and the phase noise is the lowest are 60 nm apart from each other. This is important since it is required simultaneous prominent quantum efficiency and minimal phase noise at the illumination wavelength.

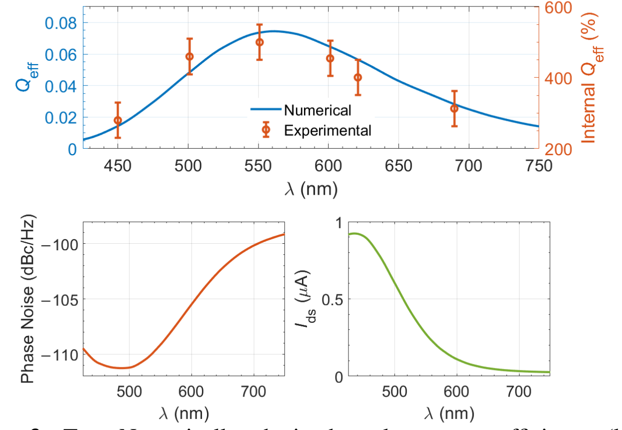

Fig. 3: Top: Numerically obtained total quantum efficiency (left y-axis) and internal quantum efficiency (right y-axis) experimentally obtained [1]. Bottom: (left) phase noise and (right) output current as a function of excitation wavelength.

The monochromatic FDTD computations take less than two minutes on a desktop computer. A more detailed analysis of the device, such as its bandwidth and how its phase noise changes with modulation frequency, will be discussed at the conference.

IV. Conclusion

In conclusion, our work addresses a critical gap in the field by introducing a sophisticated yet computationally efficient numerical model for simulating $\mathrm{MoS_2}$-based devices. The results presented herein not only contribute to the understanding of the fundamental properties of these materials but also offer practical insights for the optimization of photodetector performance.

References

[1] J. Pak *et al.*, "Intrinsic optoelectronic characteristics of $\mathrm{MoS_2}$ phototransistors via a fully transparent van der waals heterostructure," *ACS Nano*, vol. 13, no. 8, pp. 9638–9646, 2019.

[2] O. Lopez-Sanchez, D. Lembke, M. Kayci, A. Radenovic, and A. Kis, "Ultrasensitive photodetectors based on monolayer $\mathrm{MoS_2}$," *Nature Nanotechnology*, vol. 8, pp. 497–501, 2013.

[3] D. Vaquero *et al.*, "Fast response photogating in monolayer $\mathrm{MoS_2}$ phototransistors," *Nanoscale*, vol. 13, pp. 16 156–16 163, 2021.

[4] B. Mukherjee, F. Tseng, D. Gunlycke, K. K. Amara, G. Eda, and E. Simsek, "Complex electrical permittivity of the monolayer molybdenum disulfide ($\mathrm{MoS_2}$) in near UV and visible," *Opt. Mater. Express*, vol. 5, no. 2, pp. 447–455, Feb. 2015.

[5] K. H. Smithe, Kirby, C. D. English, S. V. Suryavanshi, and E. Pop, "High-field transport and velocity saturation in synthetic monolayer $\mathrm{MoS_2}$," *Nano Letters*, vol. 18, no. 7, pp. 4516–4522, 2018.

[6] A. Ueda *et al.*, "Ambipolar device simulation based on the drift-diffusion model in ion-gated transition metal dichalcogenide transistors," *NPJ Computational Materials*, vol. 6, 2020.

[7] E. Simsek, I. M. Anjum, T. F. Carruthers, C. R. Menyuk, J. C. Campbell, D. A. Tulchinsky, and K. J. Williams, "Fast evaluation of rf power spectrum of photodetectors with windowing functions," *IEEE Transactions on Electron Devices*, vol. 70, no. 7, pp. 3643–3648, 2023.